From biogas upgrading to CO_2 utilization and waste recycling: A novel circular economy approach

Francisco M. Baena-Moreno [a,b,*], Estelle le Saché [b], Cameron Alexander Hurd Price [b], T. R. Reina [b], Benito Navarrete [a].

[a] *Chemical and Environmental Engineering Department, Technical School of Engineering, University of Seville, C/ Camino de los Descubrimientos s/n, Sevilla 41092, Spain*

[b] *Department of Chemical and Process Engineering, University of Surrey, GU2 7XH Guildford, United Kingdom*

**Corresponding author.*

E-mail address: fbaena2@us.es (Francisco M. Baena-Moreno)

Abstract

Herein a novel process to synergize biogas upgrading, CO_2 utilization and waste recycling is proposed. Our study emerges as a promising strategy within the circular economy. In this work, the technical feasibility of Flue-Gas Desulfurization Gypsum as precipitant for definitely CO_2 storage is studied. The precipitation stage is evaluated through two key factors: the quality of the carbonate product and the precipitation efficiency obtained. The physicochemical characterization of the solid carbonate product was analysed by means of Raman, X-Ray diffraction and scanning electron microscopy. The precipitation efficiency is evaluated through the variation of the main precipitation parameters (temperature, molar ratio and time). For this purpose, two groups of experiments were performed. The first group was aimed to model the precipitation system through experiments designed with DesignExpert vs.12 software. The second group of experiments allows to compare our results with pure species as precipitants, as well as to validate the model designed. The physicochemical characterization performed reveals high purity calcite as product. Encouraging precipitation efficiencies were obtained, ranging from 53.09 to 80.09% (66% average). Furthermore, the model reveals a high influence of the molar ratio (3-5 times higher impact than other parameters) and low influence of temperature, which evidences the low energy consumption of the proposal. To optimize energy consumption, the model suggests 33 sets of parameters values. Examples of these values are 20ºC, 1.5 mol/mol, and 30 minutes, which allow to obtain a 72.57% precipitation efficiency. Overall, this study confirms the technical feasibility of this circular economy approach.

Keywords

Carbon Capture and Utilization; Biogas Upgrading; Waste Recycling; Circular Economy; Green Process;

1. Introduction

1.1 Background

Our era is facing the increasing challenge of greenhouse gases (GHG) reduction. GHG emissions, led by CO_2, have increased remarkably during the last decade [1]. This is considered the main cause for the global average temperature rise [2]. Thus, both developed and developing countries need to find solutions to tackle global warming [3,4]. In this line, the European Union (EU) is planning a new programme to achieve climate neutrality by 2050 [5]. According to the draft of this programme, the global strategy for EU countries will be based on three pillars: Excellent Science; Global Challenges and European Industrial Competitiveness; and Innovative Europe. Two of these pillars address the transformation of European industry towards a more sustainable production. Indeed, fostering the climate neutrality and promoting a circular – clean industry are within the main clusters included in the second pillar.

Among the different alternatives for reducing GHG emissions, the EU mentioned strategy proposes intensifying the use of biomass. Processing biomass into bio-based and renewable products allows to break-down the consumption of non-renewable resources and boost circular economy [5]. Furthermore, biomass utilization reduces the amount of waste to treat [6]. Biomass utilization alternatives can be classified into two main groups [7]: (1) direct utilization, which are those aimed to produce either both heat and electricity. Examples of these alternatives are the utilization of biomass in boilers or power stations to produce thermal energy – electricity; (2) indirect utilization, including the production of chemicals, renewable materials and/or fuels. Representative examples of this second alternative are the production of green carbon materials (i.e. biochar or hydrochar) through pyrolysis or hydrothermal carbonation [8,9], or green chemicals such as methane or formic acid [10,11]. Among biomass utilization paths, a promising alternative for biomass utilization is anaerobic digestion to produce biogas [12]. Biogas is a renewable source of energy which, if upgraded, can replace non-renewable natural gas [11]. The need of upgrading arises because biogas is composed mainly by CH_4 and CO_2 (60% - 40% approximately) [10,13]. Several biogas upgrading technologies have been proposed to date, showing outstanding results and commercial availability. These technologies are based on Carbon Capture and Storage (CCS) techniques [14]. Nonetheless, all biogas upgrading technologies share a drawback: the outcome of CO_2

upon its scrubbing from biogas. Geologic CO_2 storage implies certain risks related to leakage and seismicity. Moreover, the injected volume for reducing significantly CO_2 in the atmosphere is lofty [15].

A promising alternative to CCS technologies is Carbon Capture and Utilization (CCU) [16], which aims to use CO_2 as raw material rather than considering it a waste [17]. CCU avoids storage risks but again the CO_2 worldwide volume is overmuch to transform it all into added-value products. Nevertheless, CCU is a potential technology to synergize with biogas upgrading since the amount of CO_2 coming from biogas is quite concentrated. Moreover, this combination favours the development of negative carbon technologies as the CO_2 used is biogenic. In this line, CO_2 utilization from biogas has been the core of our research group during the last years. In previous works, we have proposed the co-production of bio-methane and calcium – magnesium carbonate from biogas. In these works, we used NaOH and KOH to absorb CO_2 (Eq. 1) in a packed tower and hence produced a high purity bio-methane stream. The resulting Na_2CO_3/K_2CO_3 is sent to a precipitation reactor in which it reacts either with a hydroxide ($Ca(OH)_2$ or $Mg(OH)_2$, Eq. (2)), or with a salt ($CaCl_2$ or $MgCl_2$) to produce a valuable solid carbonate. Our works revealed excellent results in terms of precipitation efficiency and physicochemical properties of the final carbonate.

$$2NaOH/KOH + CO_2 \rightarrow Na_2CO_3 \,/\, K_2CO_3 + H_2O \quad (1)$$

$$Na_2CO_3\,/K_2CO_3 + Ca(OH)_2/Mg(OH)_2 \rightarrow 2NaOH/KOH + CaCO_3/MgCO_3 \quad (2)$$

1.2 Goal, scope and workflow

Even though the results obtained in our previous studies were quite promising and show opportunities to scale-up the process, in all these works the precipitator used were pure species. Stepping forward to combine biogas upgrading & CO_2 utilization, we went further in our proposal and searched for a rich Ca/Mg industrial waste which could act as precipitator. As explained in our previous work [18], high Ca compounds are more favorable than Mg compounds for the precipitation reaction carried out. Thus, we focused our search on Ca-rich waste. Red gypsum is a rich Ca waste produced in Flue-Gas Desulfurization (FGD) units of coal-based power stations. In fact, it is also known as FGD Gypsum. It is composed mainly by $CaSO_4$ and can be used as raw material in cement manufacture or building plasters, among others industrial applications [19]. Nevertheless, its huge production makes unfeasible its full utilization and hence tonnes of this waste are disposed yearly. In this work, we study the potential utilization of real

red gypsum waste as precipitator in our scheme proposal (Figure 1). According to the reaction represented in Eq. (3), $CaCO_3$ can be obtained as added-value product.

$$Na_2CO_3 + CaSO_4 \rightarrow Na_2SO_4 + CaCO_3 \quad (3)$$

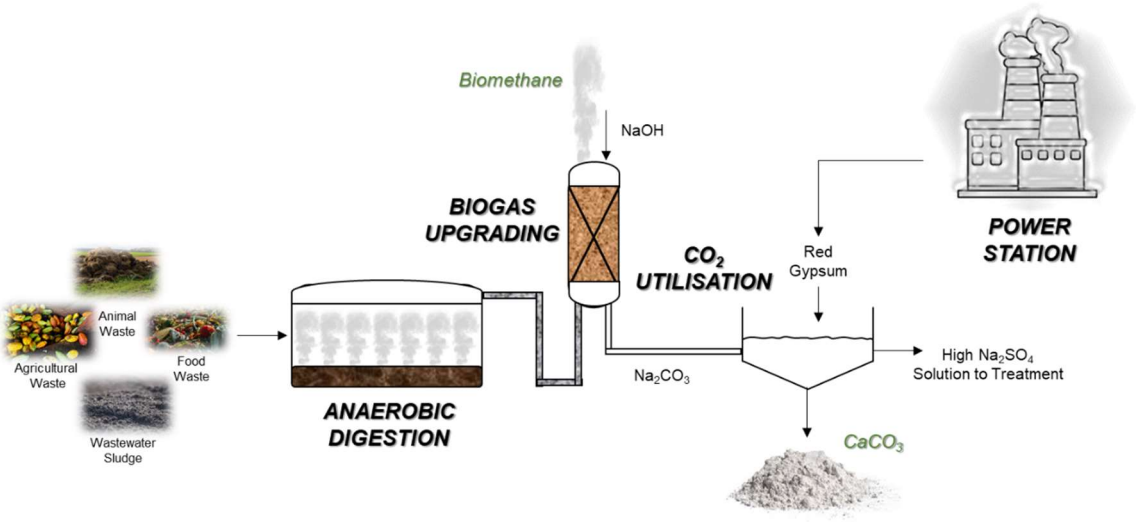

Figure 1. Biogas upgrading to CO_2 utilization and waste recycling process scheme

$CaCO_3$ can be used in numerous applications, but its price depends on the quality and carbonate type [20]. Moreover, the affordability of the process highly depends on the precipitation efficiency obtained. Therefore, the purposes of our work are both to analyse the physicochemical properties of the final $CaCO_3$ and the precipitation efficiency of this novel process. We decided to use Na_2CO_3 as carbonate carrier, which comes from the CO_2 absorbed with NaOH, since it was demonstrated in our previous works to give optimal precipitation efficiencies over K_2CO_3 [21,22]. The potential purification and valorization of the resulting Na_2SO_4 solution can be done by means membrane technology [23,24]. Indeed, commercial Na_2SO_4 crystals could be obtained using membrane distillation [25,26] or membrane nanofiltration [27]. However, as can be seen in the references cited, this fact presents no novelty as the technical viability has been already proven. Therefore, Na_2SO_4 solution valorization is out of the scope of the current work.

To meet these goals, our work is organised as follows. First, we include a complete physicochemical characterization of the powders via Raman, X-Ray diffraction (XRD) and scanning electron microscope (SEM). The combination of these three analytical techniques reveals the true nature of the solid powders obtained. Afterwards, the precipitation efficiency of $CaCO_3$ is studied through a variation of the main parameters that may affect the overall performance (reaction time, reaction temperature, and molar

ratio reactant/precipitator (R)). The present study is divided into two set of experiments: 1) The first set allows to obtain a model of the system for the selected parameters. This model can predict the precipitation efficiency within the range of values tested, quantifying the influence of reaction time, reaction temperature and R. For this purpose, an experimental design was elaborated with the software DesignExpert vs.12; 2) The second round is aimed to compare the precipitation efficiencies between the present study and our previous works. This comparison allows to evaluate the difference between pure species and industrial waste as precipitators and hence confirming the worthiness of the proposal. Furthermore, these experiments serve also to validate the model obtained.

The present study brings a breakthrough solution for combining biogas upgrading and CO_2 – waste utilization. The EU expects that these technologies transform European industries towards climate-neutral alternatives, knowing the ambitious character of this target. In this sense, our work represents a contribution to paving the way to towards zero-emissions or negative emissions technologies in a circular economy scenario.

2. Materials and Methods.

2.1 Materials

NaOH, Na_2CO_3 and $CaCO_3$ employed in this work were provided by PanReac-AppliChem (pure-grade or pharma-grade, 99% purity). The red gypsum employed in our work was provided by an industrial partner whose identity is omitted for sake of confidentiality.

2.2 Methods

Physicochemical Characterization

The solid $CaCO_3$ obtained by filtration was dried at 105°C during 24 hours. The solid was then characterized by means of SEM, XRD and Raman spectroscopy to corroborate the formation of the PCC and get some insights on its main features

Raman measurements of the powder samples were recorded using a Xplora plus spectrometer from Horiba using a 532 nm ion laser and a 50x objective.

X-ray diffraction (XRD) analysis was completed by an X'Pert Powder instrument from PAN analytical. The 2θ angle was increased by 0.05º, with a 450 time per step over a

range of 10-90º. Diffraction patterns were then recorded at 30 mA and 40 kV, using Cu Kα radiation (λ=0.154 nm).

A JEOL JSM-7100F FESEM operated at 10 KV equipped with energy dispersive X-ray spectroscopy (EDX) system was used for the microstructural/chemical characterization (SEM with EDX). The powders were coated with a thin layer of gold and positioned on a pin stub coated in colloidal graphite paint.

Experimental Study

The experimental procedure followed was the same as previously explained in our reference [28]. The values range for the parameters studied (temperature, R, and time) was also explained in our previous works [18]. For all the experiments, the initial concentration of the Na_2CO_3 – NaOH aqueous solution coming from the absorption stage was set at 20 g/100 mL Na_2CO_3 and 6 g/100 mL NaOH. The precipitation efficiency of $CaCO_3$ was defined as shown in Eq. (4), in which the maximum $CaCO_3$ corresponds to the stochiometric $CaCO_3$ produced in a complete reaction.

$$Precipitation\ efficiency\ (\%) = \frac{CaCO_3\ obtained}{CaCO_3\ maximum}\ x\ 100 \qquad (4)$$

Table 1 collects the experimental design matrix performed with the software DesignExpert vs.12. The results obtained in these tests were fitted by a mathematical model. The quality of the fit polynomial model was expressed by R^2 and its statistical significance was examined by the F-test. The space of interest follows these ranges: temperature (parameter "A") 20-80 ºC; R (parameter "B") 0.7-1.5 mol/mol; and time (parameter "C") 5-120 minutes. To provide certainty in the space of interest, DesignExpert vs.12 must go beyond the limits imposed in some tests. Examples of these tests are test 3 (R=1.56, beyond the limit of 1.5), test 8 (t=129.9 minutes, beyond the limit of 120 minutes) and test 9 (temperature of 15.2ºC, beyond the limit of 20ºC).

Table 1. Experimental design matrix for the first round of experiments

Test	A: T (ºC)	B: R (mol/mol)	C: t (min)
1	28.9	0.94	98.9
2	70	1.15	67.5
3	42.6	1.56	67.5
4	28.9	0.94	98.7
5	56.3	0.94	36.2
6	42.6	0.73	67.5
7	56.3	0.94	98.7
8	42.6	1.15	129.9

9	15.2	1.15	67.5
10	42.6	1.15	67.5
11	42.6	1.15	67.5
12	56.3	1.35	36.2
13	56.3	0.94	36.2
14	56.3	1.35	98.7
15	28.9	1.35	36.2
16	56.3	0.94	98.7
17	42.6	1.15	67.5
18	28.9	1.35	98.7
19	42.6	1.15	67.5
20	42.6	1.15	67.5
21	56.3	1.35	98.7
22	28.9	1.35	98.7
23	28.9	1.35	36.2
24	28.9	0.94	36.2
25	42.6	1.15	67.5
26	28.9	0.94	36.2
27	56.3	1.35	36.2
28	42.6	1.15	5.1

Table 2 shows the matrix of experiments carried out in the second round. As previously explained, these experiments served to evaluate the precipitation efficiency differences between pure species and waste. The values chosen for temperature, R and time were the most representative ones to compare with previous studies [29]. The parameters chosen for test 1 were considered as standard in agreement with previous references [30,31]. Reproducibility checks were conducted for all the experiments, resulting in an overall experimental error of ±2% for the precipitation efficiency.

Table 2. Matrix of experiments carried out in the second round

Test	T (ºC)	R (mol/mol)	t (min)
29*	50	1.2	30
30	30	1.2	30
31	70	1.2	30
32	50	1	30
33	50	1.5	30
34	50	1.2	15
35	50	1.2	60

***Standard test**

3. Results

3.1 PCC Physicochemical Characterization Results

Raman measurements

The physicochemical characterization of the powders sample is crucial to know the commercial quality of the product and hence to evaluate the feasibility of the process. Albeit all the samples were measured obtaining identical results, for sake of clarity the

results showed in this section are based on the powders obtained in test 1 (standard). The first step to characterize the powder samples obtained was to corroborate the presence of carbonates. In this sense, Raman spectroscopy is a powerful tool to get information about species contained in a powder sample. Figure 2 shows the results obtained for the Raman analysis on the initial waste sample and the sample obtained in the standard test. Figure 2.A reveals a typical gypsum composition in the waste sample. The main band of gypsum spectra appears at 1010 cm^{-1}, belonging to the v_1 symmetric stretch vibration mode of the SO_4 tetrahedra [32]. The minor bands (415, 495, 622, 674, and 1143 cm^{-1}) presented in Figure 2.A further confirm the gypsum nature of the waste samples [33]. The Raman spectra of the solid particles resulting from the precipitation experiments are plotted in Figure 2.B. The spectra obtained confirms the success of the experiments performed. The most characteristic band of $CaCO_3$ appears at 1088 cm^{-1}. As plotted in Figure 2.B this band is present in the powder obtained in our experiments (blue line), which agrees with the monoclinic structure of P21/c group. Indeed, the solid obtained presents the same spectra than a commercial $CaCO_3$ sample (green line). Indeed Raman spectra exhibits three main peaks that are related to vibrations within the carbonate moiety [34]. The peak at 1088 cm^{-1} corresponds to the v_1 symmetric stretch while the peak at 711 cm^{-1} corresponds to v_4 the in-plan bending of the carbonate [34]. The peak at 301 cm^{-1} on the other hand is related to a lattice mode [34], characteristic of a calcite structure, although these results will be further confirmed by XRD analysis.

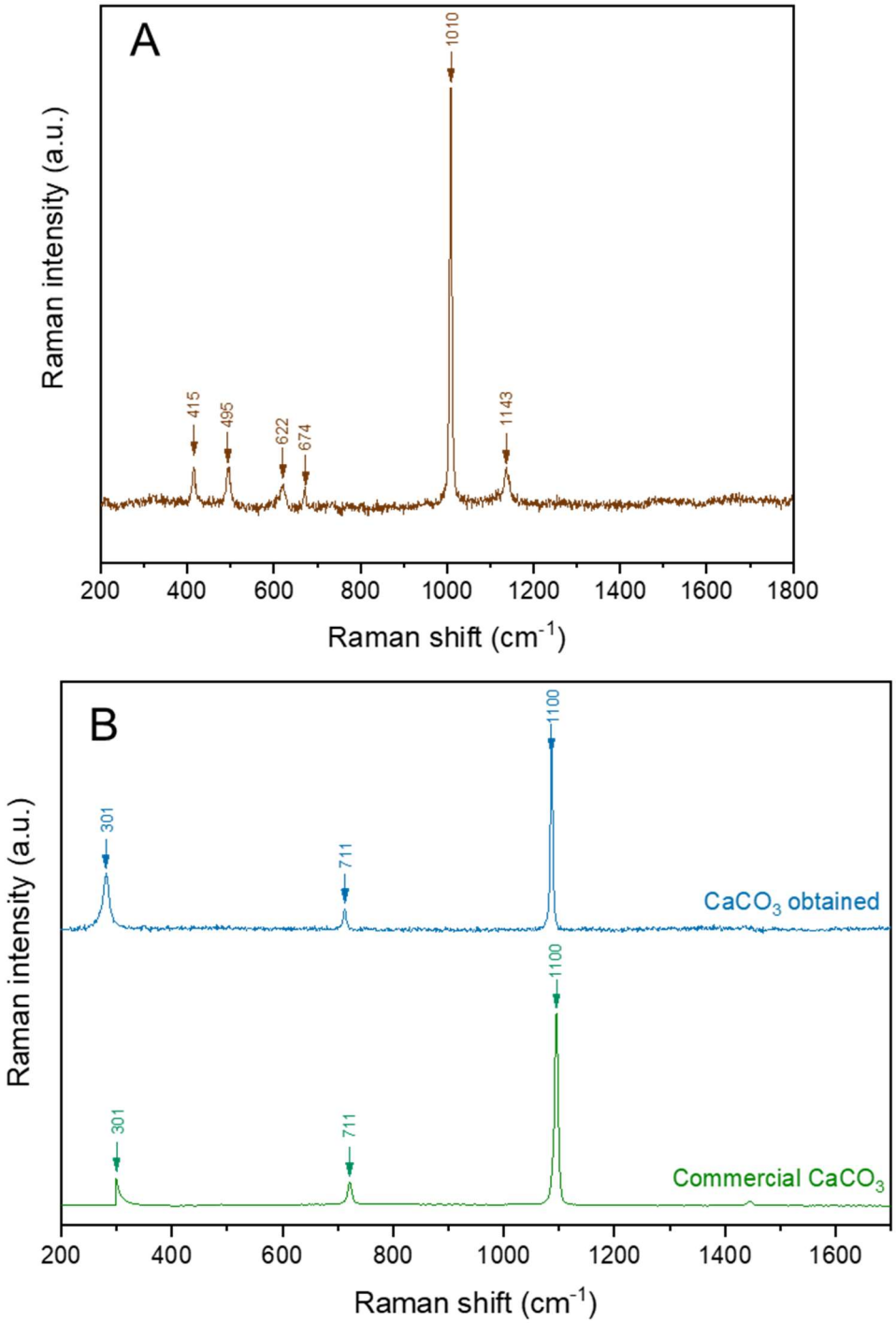

Figure 2. Raman spectra for: A: red gypsum waste and; B: for $CaCO_3$ obtained (standard test) and commercial $CaCO_3$.

XRD analysis

The potential use of $CaCO_3$ strongly depends on the crystal morph. XRD allows to ascertain the crystal structure of solid samples. Therefore, both the waste and the powders obtained were analysed by means of this technique. Figure 3.A shows the XRD patterns of the initial waste. $CaSO_4$ can be found in three different morphs: anhydrite, bassanite, and gypsum [35]. These morphs differ from each other in the amount of water contained in the crystal structure. Some of the peaks presented in the anhydrite and gypsum patterns can be similar [36]. As shown in Figure 3.A, the waste herein employed as precipitator presents the characteristic features of gypsum as the major phase and traces of the hydrated polymorphs. Regarding the product obtained, Figure 3.B depicts the XRD pattern and its comparison with a commercial sample of calcite. As observed, the patterns are identical and hence calcite can be confirmed as the product obtained. Calcite is the most stable form of $CaCO_3$ and it is recognisable by its intense peak at 28° [37]. The potential applications of calcite are extensive, being more typically employed in pharmacy, cement, paper and polymers industry. Therefore, our carbonate can fit in the industrial market, showing promising characteristics as added-value product. The XRD patterns of the both powders (waste and $CaCO_3$ obtained) allows to conclude that a complete transformation was achieved in our precipitation experiments.

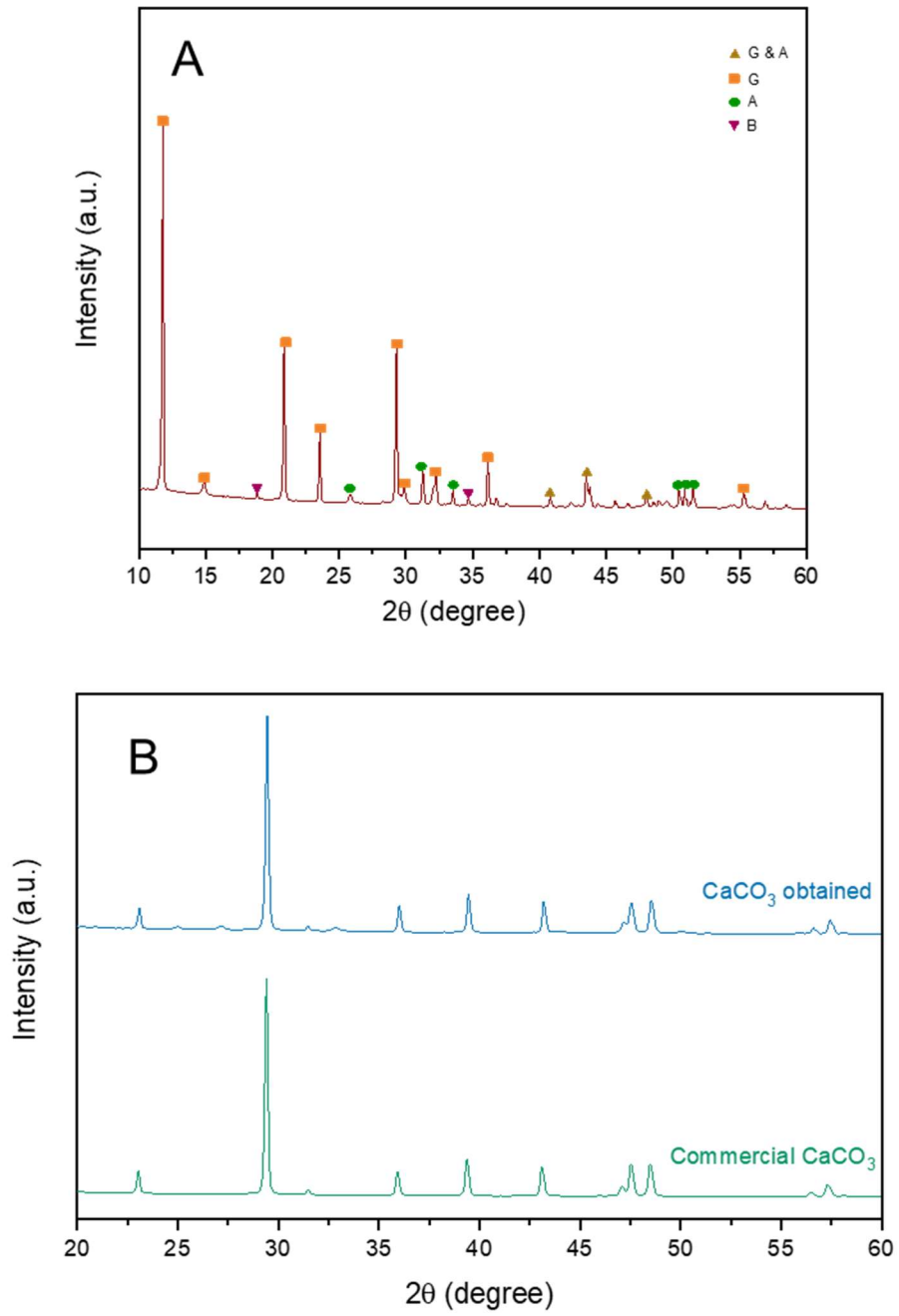

Figure 3. XRD diffractogram of: A: the initial waste (G & A: Gypsum & Anhydrite; G: Gypsum; A: Anhydrite; B: Bassanite.) and; B: $CaCO_3$ obtained (standard test) and commercial calcite.

SEM-EDX analysis

SEM analysis is a powerful tool to gain some insights of the solid particles morphology. Furthermore, EDX analysis allows to further examine the composition of the solid obtained, ensuring that the final product is not contaminated with minor impurities.

Figures 4 and 5 show the SEM images of the red gypsum waste and the $CaCO_3$ product, respectively. The red gypsum morphology observed in Figure 4 corresponds to the typical prismatic crystal structure [38]. Concerning the morphology of the final $CaCO_3$ product showed in Figure 5, it matches with the tetrahedral morphology of calcite. This results further confirms our hypothesis forwarded in XRD analysis [20]. On the other hand, Table 3 collects the results of the EDX analysis. We observe the existence of minor impurities in the red gypsum waste (0.1% of Mg and 0.1% of Al). The appearance of these elements may be caused by impurities dragged from previous stages to FGD. Nonetheless, these impurities do not appear in the final solid sample, confirming once more the high quality of the product obtained.

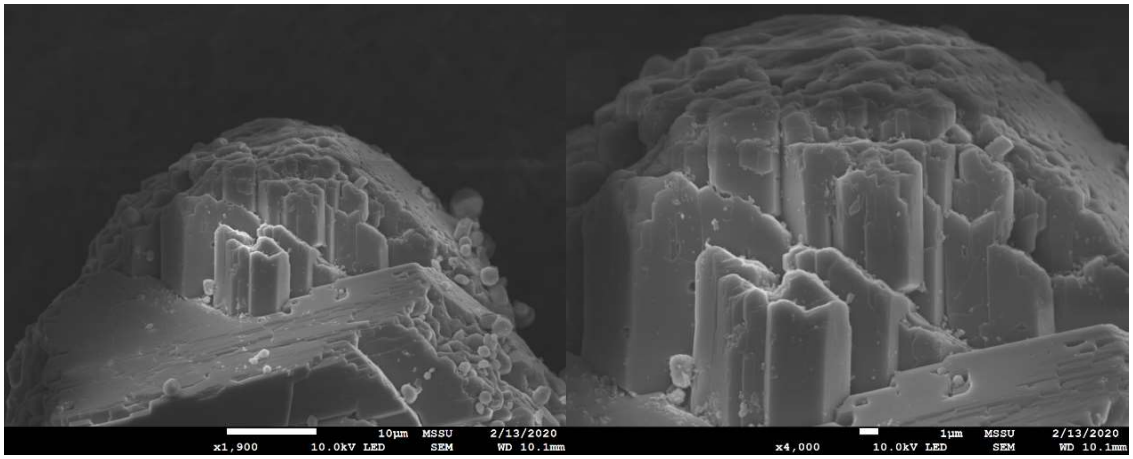

Figure 4. SEM images of the initial red gypsum waste

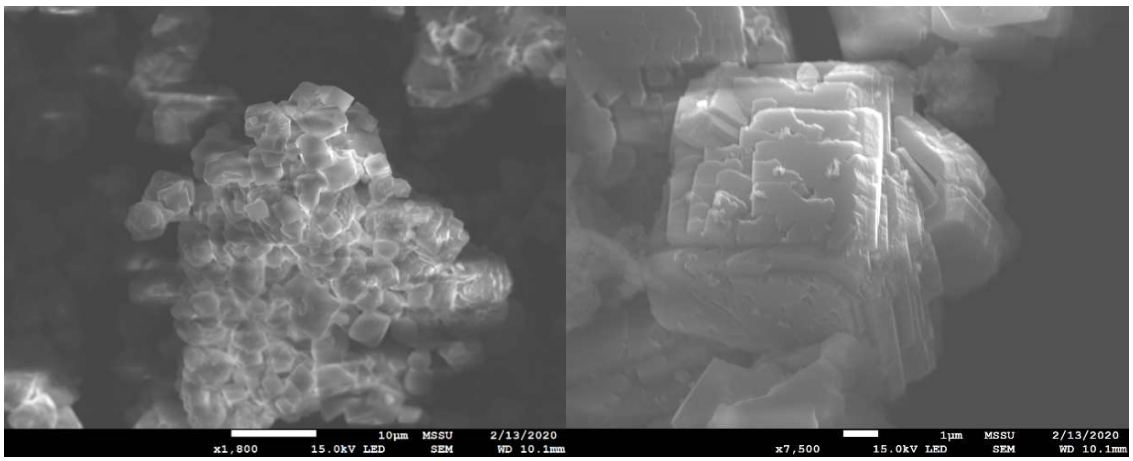

Figure 5. SEM images of the $CaCO_3$ obtained in the standard test.

Table 3. EDX results

Element	Red gypsum (%)	$CaCO_3$ product (%)

C	-	6.5
O	58.8	62.1
Ca	22.2	31.4
S	18.8	-
Al	0.1	-
Mg	0.1	-

3.2 Precipitation results

Model results and analysis

To quantify the influence of temperature, reaction time and R ratio, 28 experiments were performed and Figure 6 shows the precipitation efficiency obtained in every case. As depicted, the results obtained range from 53.09% to 80.09%, which confirms a high influence of the parameters studied.

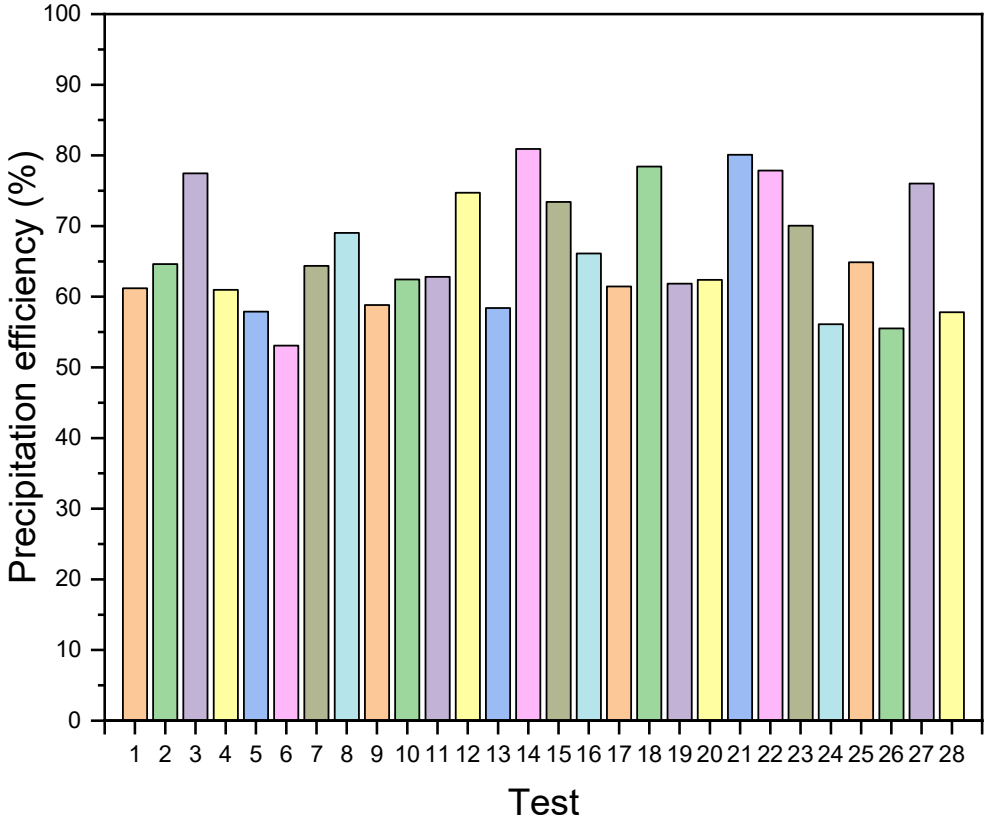

Figure 6. Precipitation efficiency obtained for the tests carried out in the first set.

The results presented in Figure 6 allowed to draw a mathematical model (Eq. (5) for actual factors and Eq. (6) for code factors) for the precipitation efficiency system. Table

4 collects the precipitation efficiency model statistics. As shown, the linear model is suggested as it presents the higher correlation coefficients (R^2). The model's F-value (52.97) and the p-values (<0.05) ensure that the mathematical model obtained is significant and hence it can be used to predict the precipitation efficiency in the range of study. Figure 7 shows the differences between predicted values according to the linear model and actual values obtained through experiments.

$$Prec.Efficiency\,(\%) = 13.58252 + 0.111365 \cdot T + 35.96445 \cdot R + 0.093793 \cdot t \quad (5)$$

$$Prec.Efficiency\,(\%) = 64.81 + 3.34 \cdot A + 14.39 \cdot B + 5.16 \cdot C \quad (6)$$

Table 4. Precipitation efficiency model statistics

Source	**Sequential p-value**	**Lack of Fit p-value**	**Adjusted R²**	**Predicted R²**	**Comment**
Linear	< 0.0001	< 0.0001	0.8524	0.8223	Suggested
2FI	0.9988	< 0.0001	0.8315	0.7727	
Quadratic	0.2275	< 0.0001	0.8445	0.5945	
Source	**Sum of Squares**	**df**	**Mean Square**	**F-value**	**p-value**
Model	1605.92	3	535.31	52.97	< 0.0001
A-Temperature	55.72	1	55.72	5.51	0.0274
B-R	1344.45	1	1344.45	133.04	< 0.0001
C-Time	205.74	1	205.74	20.36	0.0001

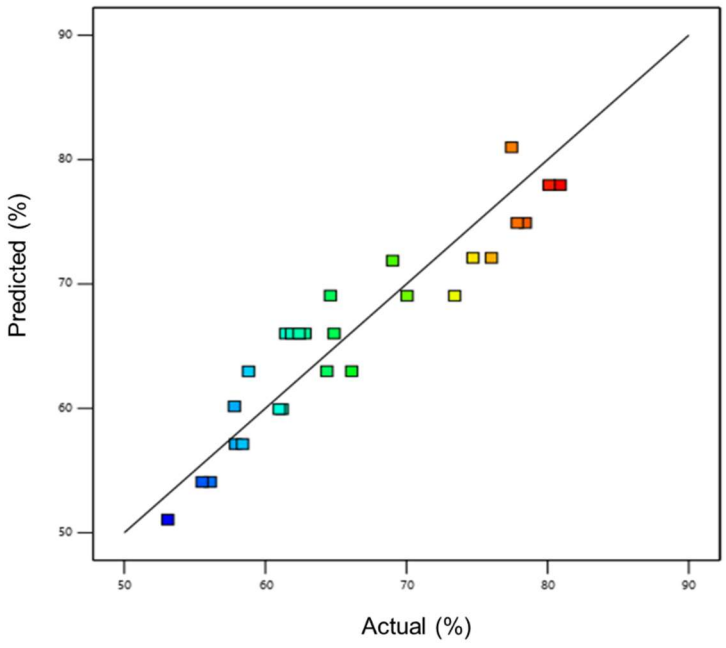

Figure 7. Predicted values vs Actual values.

As observed in Eq. (6), the parameter with a higher impact over the precipitation system is R (B). Indeed, the coefficient of this code factor is almost 3 times higher than the coefficient of second more impacting parameter. Increasing R value may seem a good strategy to obtain a better precipitation efficiency. Nonetheless, a higher R value also entails a further treatment of the liquid Na_2SO_4 solution. This balance is an interesting point to be considered in future works. Keeping on the analysis of this equation, the reaction temperature presents the lowest influence of the precipitation parameters. This is an encouraging result, as the energy consumption can be optimised without a strong penalisation of the precipitation efficiency. Finally, the reaction time may need optimisation to determine a convenient value, as a higher reaction time implies higher reactor volume in a hypothetical industrial application. Figure 8 further supports the effects of each parameter on the precipitation efficiency through the one factor model graphs. As shown, the slope of the R graph is considerably sleeper in comparison with the other two graphs.

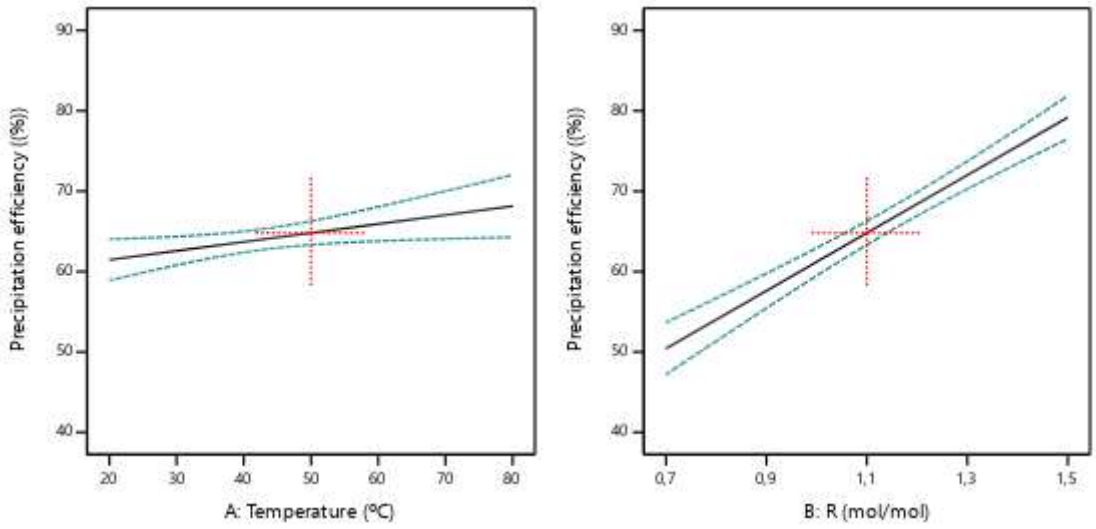

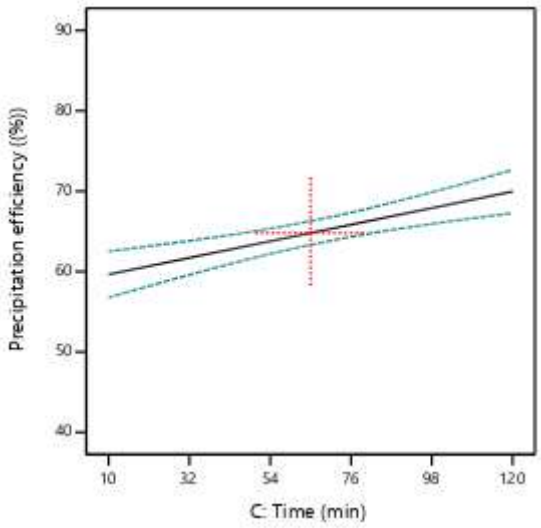

Figure 8. One factor model graphs for the precipitation efficiency system.

The response surfaces obtained for the pairs R-Temperature, Time-Temperature and Time-R are included in Figure 9. As shown these relations are also linear models, affecting the three reaction parameters positively to the precipitation efficiency. The pairs with R (Figures 9.A and 9.C) presents higher slope, which further confirms the higher influence of this parameter as discussed above. In comparison with previous works, this fact agrees well with the results obtained by Chen et al. [39]. In their work, increasing the concentration of precipitant led to considerable higher precipitation efficiencies, while keeping constant the rest of parameters. As for the poor effect of temperature, our results also match with similar previous studies [39,40]. For example, Li et al. obtained 20ºC as best reaction temperature for the precipitation system [41].

Comparing the precipitation efficiency values obtained with other works in which waste has been used as precipitant agent, our results are quite promising. For example, Morone et al. achieved a precipitation efficiency of around 60% of equivalent efficiency, which is lower than our average (66%) [42]. Air pollution control (APC) solid waste was also tested as precipitant agent, giving an average efficiency of 65% but after a pretreatment of the APC waste [30]. In our work similar efficiency is obtained, but no pretreatment is needed although it will be considered in future works. Waste from argon oxygen decarburization (AOD) were also employed, revealing poor efficiencies (average 15%) in comparison with our work [30].

The response surfaces also allow to optimize the precipitation efficiency. For example, if we pursue a low energy consumption, temperature must be minimized. The created

model enables to find the optimal solutions for this assumption, varying the other two parameters. In this case, 33 solutions are offered. Among them, the suggested one has the following values: 20ºC, 1.5 mol/mol, and 30 min. Under these values, the precipitation efficiency predicted is 72.57%. As demonstrated, the model designed has a lot of potential to further develop in future works.

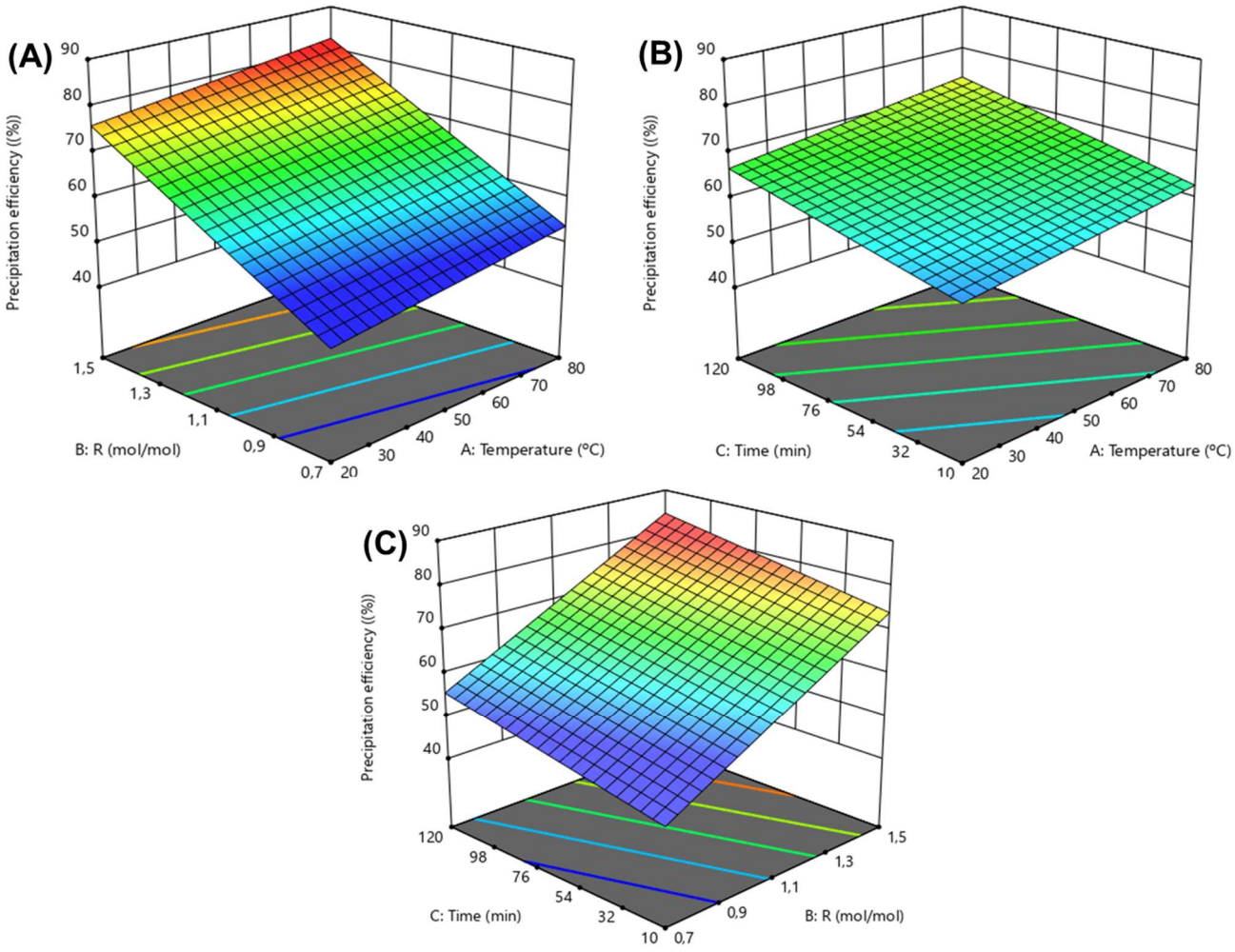

Figure 9. Response surfaces for: R-Temperature (A); Time-Temperature (B); and Time-R (C).

Comparison with pure species and model validation

For sake of comparison with our previous works, where we used pure species as precipitant agents, we performed 7 additional tests. The results are depicted in Figures 10, 11 and 12. These Figures also permit further confirmation of the influence of each precipitation parameter. Overall the precipitation efficiencies obtained with FGD Gypsum are lower than those for pure species. For instance, for the standard conditions defined, the difference is 16.49% vs $Ca(OH)_2$ and 12.89% vs $CaCl_2$. These results invite to think about potential pretreatments of the FGD Gypsum that could enhance the efficiencies, fact that will be targeted in future works.

In contrast with $Ca(OH)_2$, where the temperature plays a key role for the precipitation efficiency, for FGD gypsum and $CaCl_2$ a low temperature value is recommended. As shown in Figure 10, increasing this value does not provide a remarkable increase of the precipitation efficiency. This difference between $Ca(OH)_2$ and the other precipitants may be the consequence of the low solubility of $Ca(OH)_2$. Overall, at the low temperature values tested in our system, the efficiency differences between FGD Gypsum and the pure species are reduced under the standard conditions.

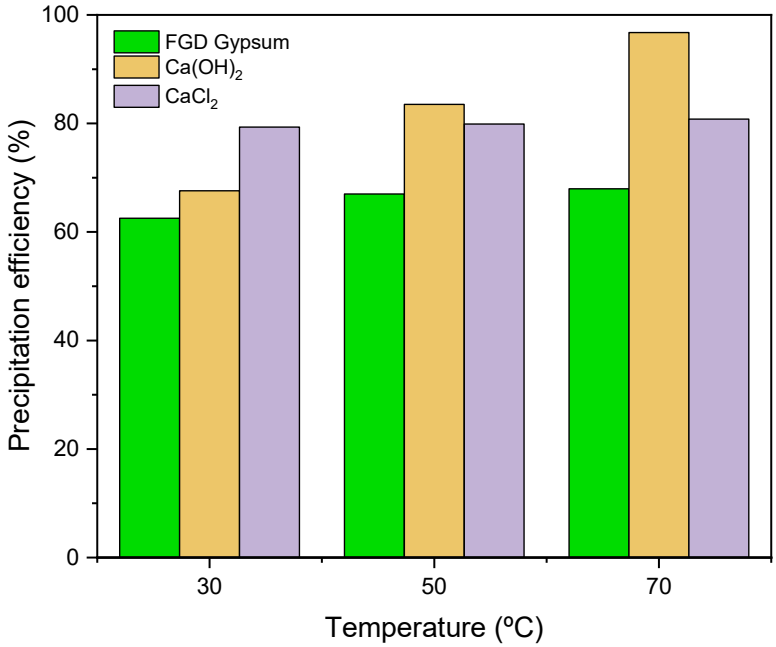

Figure 10. Temperature influence on precipitation efficiency. Comparison between FGD Gypsum and pure species at t=30min and R=1.2.

As shown in Figure 11, the influence of R values is similar for FGD Gypsum and $CaCl_2$. This result, along with the temperature influence previously analysed, suggests that FGD Gypsum display a similar behaviour than $CaCl_2$ as precipitant. In fact, increasing R value promotes a noticeable increase in the precipitant efficiency of both agents. On the contrary, increasing R hardly affects the efficiency obtained with $Ca(OH)_2$.

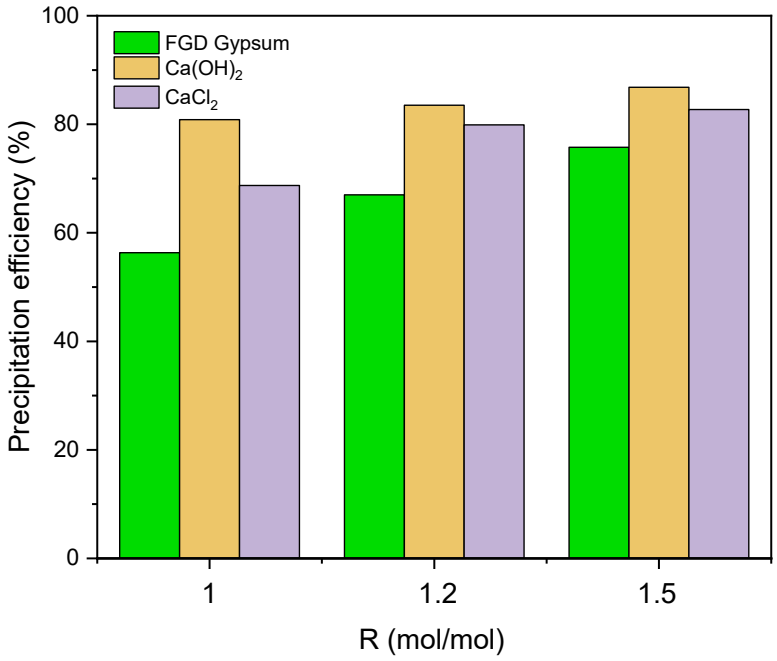

Figure 11. R influence on precipitation efficiency. Comparison between FGD Gypsum and pure species at T=50ºC and t=30min.

Finally, the effect of reaction time and the comparison between FGD Gypsum and pure species is shown in Figure 12. As in the case of temperature, the reaction time affects harder the precipitant $Ca(OH)_2$. The effect on FGD Gypsum and $CaCl_2$ follows similar trends that the ones previously explained. Thus, this result further confirms the similitudes between FGD Gypsum and $CaCl_2$ as precipitants.

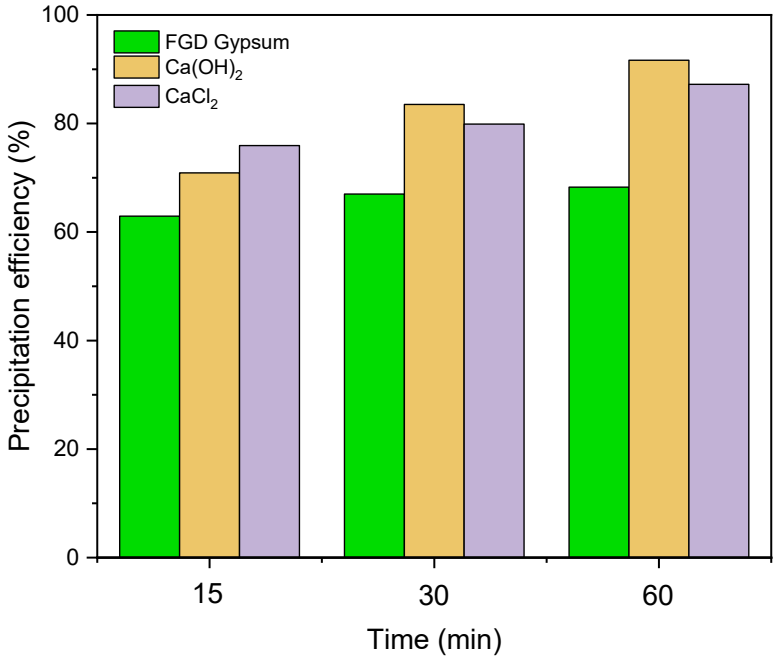

Figure 12. Time influence on precipitation efficiency. Comparison between FGD Gypsum and pure species at T=50ºC and R=1.2.

These tests also serve to validate our model above presented. In this sense, Figure 13 presents the comparison between the actual (obtained) and the predicted precipitation efficiencies. As shown, the model is very useful to accurately predict the precipitation efficiency of our system. The maximum difference found was in test 1 (standard conditions), where a 1.88% difference was obtained. A barely 2% error is an acceptable value to consider in the future scale-up and optimization of the process.

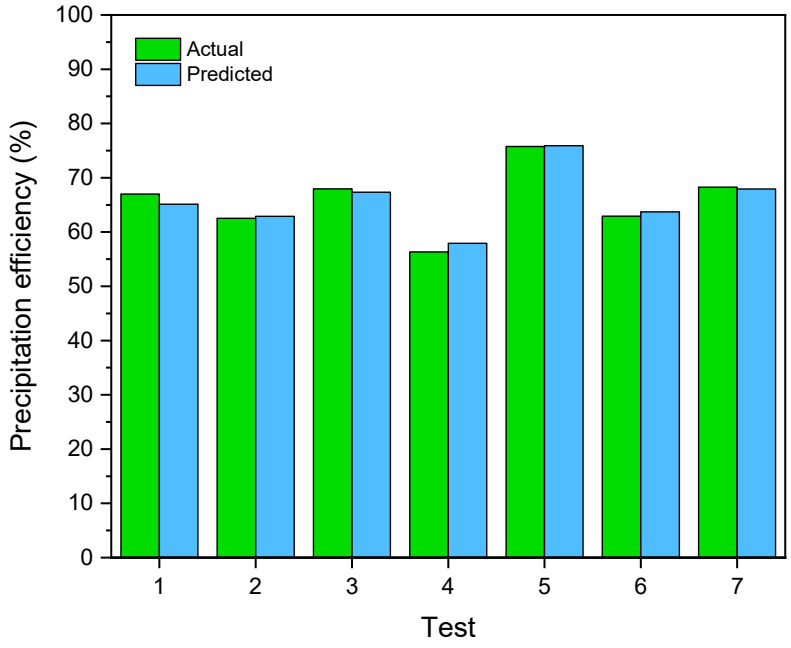

Figure 13. Difference between actual and predicted precipitation efficiencies.

4. Conclusions

This work presents the technical feasibility of a novel process to synergize biogas upgrading, CO_2 utilization and waste recycling. FGD Gypsum with high calcium content from a power station was selected as precipitant to obtain $CaCO_3$ as added value product of the CO_2 utilization process. Our approach fits well within the EU circular economy roadmap and reports for the first time both the product quality and the influence of precipitation parameters through a model designed with DesignExpert vs.12. This model allows to quantify the influence of temperature, R and time over the precipitation efficiency. Furthermore, the model allows to predict the precipitation efficiency within a range of the aforementioned parameters values.

The physicochemical characterization reveals that the $CaCO_3$ product obtained from waste is high purity calcite. Calcite has many applications and its production from these wastes is an important step in the circular economy concept. Overall the precipitation efficiency obtained is quite promising (66% average). Indeed, our results are better than the previously reported in the literature for waste precipitation. The model obtained showcases the great importance of R over temperature and time. The influence on the precipitation efficiency of this parameter is 3-5 times higher than the others. In

comparison with pure species, FGD Gypsum presents lower precipitation efficiencies than $Ca(OH)_2$ and $CaCl_2$.

Taking everything into consideration, our work has confirmed the technical feasibility of the process proposed, opening a new route for research in sustainable energy process. Further innovations in this research area are necessary to improve the efficiency and the profitability of renewable energy vectors such as bio-methane. In agreement with the results obtained here, the techno-economic analysis and the scale-up of the process will be the subject of future works. These future works will also deal with the valorization of the resulting Na_2SO_4 through the technologies described before. Moreover, the inclusion of some waste pre-treatments into the process scheme which may enhance the precipitation efficiency will be analysed.

Acknowledgments and Funding

This work was supported by EMASESA through NURECCO2 project and Corporación Tecnológica de Andalucía (CTA). Moreover this work was supported by University of Seville through V PPIT-US. Financial support for this work was also provided by the EPSRC grant EP/R512904/1 as well as the Royal Society Research Grant RSGR1180353. Furthermore this work was also partially sponsored by the CO_2Chem UK through the EPSRC grant EP/P026435/1, and the Spanish Ministry of Science and Innovation through the project RYC2018-024387-I.

References

[1] G. Boden, T. A.; Andres, R. J.; Marland, Global, Regional, and National Fossil-Fuel CO2 Emissions (1751 - 2014), 2017. doi:doi:10.3334/CDIAC/00001_V2017.

[2] H. Ritchie, M. Roser, CO_2 and Greenhouse Gas Emissions, Our World Data. (2020).

[3] S. Kumar, R. Srivastava, J. Koh, Utilization of zeolites as CO2 capturing agents: Advances and future perspectives, J. CO2 Util. (2020). doi:10.1016/j.jcou.2020.101251.

[4] E. Le Saché, L. Pastor-Pérez, B.J. Haycock, J.J. Villora-Picó, A. Sepúlveda-Escribano, T.R. Reina, Switchable Catalysts for Chemical CO2 Recycling: A Step Forward in the Methanation and Reverse Water-Gas Shift Reactions, ACS Sustain. Chem. Eng. (2020). doi:10.1021/acssuschemeng.0c00551.

[5] Europe Union, Orientations towards the first Strategic Plan for Horizon Europe, 2019.

[6] E. Uggetti, B. Sialve, J. Hamelin, A. Bonnafous, J.P. Steyer, CO2 addition to increase biomass production and control microalgae species in high rate algal ponds treating wastewater, J. CO2 Util. (2018). doi:10.1016/j.jcou.2018.10.009.

[7] P. Mizsey, L. Racz, Cleaner production alternatives: Biomass utilisation options, J. Clean. Prod. (2010). doi:10.1016/j.jclepro.2010.01.007.

[8] J. González-Arias, M.E. Sánchez, E.J. Martínez, C. Covalski, A. Alonso-Simón, R. González, J. Cara-Jiménez, Hydrothermal carbonization of olive tree pruning as a sustainableway for improving biomass energy potential: Effect of reaction parameters on fuel properties, Processes. (2020). doi:10.3390/PR8101201.

[9] R. González, J. González, J.G. Rosas, R. Smith, X. Gómez, Biochar and Energy Production: Valorizing Swine Manure through Coupling Co-Digestion and Pyrolysis, C — J. Carbon Res. 6 (2020) 43. doi:10.3390/c6020043.

[10] F.M. Baena-Moreno, D. Sebastia-Saez, Q. Wang, T.R. Reina, Is the production of biofuels and bio-chemicals always profitable? Co-production of biomethane and urea from biogas as case study, Energy Convers. Manag. (2020). doi:10.1016/j.enconman.2020.113058.

[11] F.M. Baena-Moreno, L. Pastor-Pérez, Z. Zhang, T.R. Reina, Stepping towards a low-carbon economy. Formic acid from biogas as case of study, Appl. Energy. 268 (2020). doi:10.1016/j.apenergy.2020.115033.

[12] Y. Kathiraser, Z. Wang, M.L. Ang, L. Mo, Z. Li, U. Oemar, S. Kawi, Highly active and coke resistant Ni/SiO2catalysts for oxidative reforming of model biogas: Effect of low ceria loading, J. CO2 Util. (2017). doi:10.1016/j.jcou.2017.03.018.

[13] A. Catarina Faria, C. V. Miguel, L.M. Madeira, Thermodynamic analysis of the CO2 methanation reaction with in situ water removal for biogas upgrading, J. CO2 Util. (2018). doi:10.1016/j.jcou.2018.05.005.

[14] R.M. Cuéllar-Franca, A. Azapagic, Carbon capture, storage and utilisation technologies: A critical analysis and comparison of their life cycle environmental impacts, J. CO2 Util. 9 (2015) 82–102. doi:10.1016/j.jcou.2014.12.001.

[15] S.T. Anderson, Risk, Liability, and Economic Issues with Long-Term CO2

Storage—A Review, Nat. Resour. Res. (2017). doi:10.1007/s11053-016-9303-6.

[16] V. Rodin, J. Lindorfer, H. Böhm, L. Vieira, Assessing the potential of carbon dioxide valorisation in Europe with focus on biogenic CO2, J. CO2 Util. (2020). doi:10.1016/j.jcou.2020.101219.

[17] B. Han, G. Wei, R. Zhu, W. Wu, J.J. Jiang, C. Feng, J.F. Dong, S.Y. Hu, R.Z. Liu, Utilization of carbon dioxide injection in BOF-RH steelmaking process, J. CO2 Util. (2019). doi:10.1016/j.jcou.2019.05.038.

[18] F.M. Baena-Moreno, M. Rodríguez-Galán, T.R. Reina, Z. Zhang, L.F. Vilches, B. Navarrete, Understanding the effect of Ca and Mg ions from wastes in the solvent regeneration stage of a biogas upgrading unit, Sci. Total Environ. (2019). doi:10.1016/j.scitotenv.2019.07.135.

[19] E. Petavratzi, S. Wilson, Characterisation of Mineral Wastes , Resources and Processing technologies – Integrated waste management for the production of construction material WRT 177 / WR 0115 Case Study : Waste mineral fibre in ceiling tile manufacture, 2007.

[20] F.M. Baena-Moreno, M. Rodríguez-Galán, F. Vega, T.R. Reina, L.F. Vilches, B. Navarrete, Synergizing carbon capture storage and utilization in a biogas upgrading lab-scale plant based on calcium chloride: Influence of precipitation parameters, Sci. Total Environ. (2019). doi:10.1016/j.scitotenv.2019.03.204.

[21] F.M. Baena-Moreno, F. Vega, L. Pastor-Pérez, T.R. Reina, B. Navarrete, Z. Zhang, Novel process for carbon capture and utilization and saline wastes valorization, J. Nat. Gas Sci. Eng. (2020). doi:10.1016/j.jngse.2019.103071.

[22] F.M. Baena-Moreno, M. Rodríguez-Galán, F. Vega, T. Ramirez-Reina, L. Vilches, B. Navarrete, Understanding the influence of the alkaline cation K+ or Na+ in the regeneration efficiency of a biogas upgrading unit, Int. J. Energy Res. (2019) 1–8. doi:10.1002/er.4448.

[23] M.T. Chan, A.G. Fane, J.T. Matheickal, R. Sheikholeslami, Membrane distillation crystallization of concentrated salts - Flux and crystal formation, J. Memb. Sci. (2005). doi:10.1016/j.memsci.2004.09.051.

[24] Y. Choi, G. Naidu, S. Lee, S. Vigneswaran, Recovery of sodium sulfate from seawater brine using fractional submerged membrane distillation crystallizer, Chemosphere. (2020). doi:10.1016/j.chemosphere.2019.124641.

[25] R. Bouchrit, A. Boubakri, T. Mosbahi, A. Hafiane, S.A.T. Bouguecha, Membrane crystallization for mineral recovery from saline solution: Study case Na2SO4 crystals, Desalination. (2017). doi:10.1016/j.desal.2017.02.021.

[26] C.A. Quist-Jensen, F. Macedonio, D. Horbez, E. Drioli, Reclamation of sodium sulfate from industrial wastewater by using membrane distillation and membrane crystallization, Desalination. (2017). doi:10.1016/j.desal.2016.05.007.

[27] F. Jia, J. Wang, Treatment of flue gas desulfurization wastewater with near-zero liquid discharge by nanofiltration-membrane distillation process, Sep. Sci. Technol. (2018). doi:10.1080/01496395.2017.1379539.

[28] F.M. Baena-Moreno, M. Rodríguez-Galán, F. Vega, T.R. Reina, L.F. Vilches, B. Navarrete, Regeneration of Sodium Hydroxide from a Biogas Upgrading Unit through the Synthesis of Precipitated Calcium Carbonate: An Experimental Influence Study of Reaction Parameters, Processes. 6 (2018). doi:10.3390/pr6110205.

[29] R. Baciocchi, E. Carnevale, G. Costa, R. Gavasci, L. Lombardi, T. Olivieri, L. Zanchi, D. Zingaretti, Performance of a biogas upgrading process based on alkali absorption with regeneration using air pollution control residues, Waste Manag. 33 (2013) 2694–2705. doi:10.1016/j.wasman.2013.08.022.

[30] R. Baciocchi, A. Corti, G. Costa, L. Lombardi, D. Zingaretti, Storage of carbon dioxide captured in a pilot-scale biogas upgrading plant by accelerated carbonation of industrial residues, Energy Procedia. 4 (2011) 4985–4992. doi:10.1016/j.egypro.2011.02.469.

[31] L. Lombardi, R. Baciocchi, E. Carnevale, A. Corti, Investigation of an innovative process for biogas up-grading – pilot plant preliminary results, Proc. ECOS 2012- 25th Int. Conf. Effic. Cost, Optim. Simul. Environ. Impact Energy Syst. June 26-29, Perugia, Italy. (2012) 1–12.

[32] N. Buzgar, A. Buzatu, I.V. Sanislav, The Raman study on certain sulfates, Analele Stiint. Ale Univ. " Al. I. Cuza" Din Iasi , Geol. (2009).

[33] N. Prieto-Taboada, O. Gómez-Laserna, I. Martínez-Arkarazo, M.Á. Olazabal, J.M. Madariaga, Raman spectra of the different phases in the CaSO4-H2O system, Anal. Chem. (2014). doi:10.1021/ac501932f.

[34] B. Xu, A. Hirsch, L. Kronik, K.M. Poduska, Vibrational properties of isotopically

enriched materials: the case of calcite, RSC Adv. (2018). doi:10.1039/C8RA06608F.

[35] B. Lafuente, J.L. Bishop, L.K. Fenton, S.J. King, D. Blake, P. Sarrazin, R.T. Downs, B.H. Horgan, Mineralogical characterization by XRD of gypsum dunes at White Sands National Monument and application to gypsum detection on Mars, in: 45th Lunar Planet. Sci. Conf., 2014.

[36] S. Ashrit, P.K. Banerjee, R. V. Chatti, R. Venugopal, G. Udayabhanu, Characterization of gypsum synthesized from LD slag fines generated at a waste recycling plant of a steel plant, New J. Chem. (2015). doi:10.1039/c4nj02023e.

[37] M. Altiner, M. Yildirim, Production of precipitated calcium carbonate particles with different morphologies from dolomite ore in the presence of various hydroxide additives, Physicochem. Probl. Miner. Process. (2017). doi:10.5277/ppmp170133.

[38] A. Azdarpour, M. Afkhami Karaei, H. Hamidi, E. Mohammadian, B. Honarvar, CO2 sequestration through direct aqueous mineral carbonation of red gypsum, Petroleum. (2018). doi:10.1016/j.petlm.2017.10.002.

[39] G. Chen, X. Song, C. Dong, S. Sun, Z. Sun, J. Yu, Mineralizing CO2as MgCO3·3H2O Using Abandoned MgCl2Based on a Coupled Reaction-Extraction-Alcohol Precipitation Process, Energy and Fuels. (2016). doi:10.1021/acs.energyfuels.6b01297.

[40] M. Arti, M.H. Youn, K.T. Park, H.J. Kim, Y.E. Kim, S.K. Jeong, Single process for CO2capture and mineralization in various alkanolamines using calcium chloride, Energy and Fuels. (2017). doi:10.1021/acs.energyfuels.6b02448.

[41] Y. Li, X. Song, G. Chen, Z. Sun, Y. Xu, J. Yu, Preparation of calcium carbonate and hydrogen chloride from distiller waste based on reactive extraction–crystallization process, Chem. Eng. J. (2015). doi:10.1016/j.cej.2014.12.058.

[42] M. Morone, G. Costa, A. Polettini, R. Pomi, R. Baciocchi, Valorization of steel slag by a combined carbonation and granulation treatment, Miner. Eng. (2014). doi:10.1016/j.mineng.2013.08.009.